Behaviour of Carbon Steel in the Presence of Hydrocarbon and a Pyridinic Compound

L. D. López León[1], M. A. Veloz Rodríguez[1,], V. E. Reyes Cruz[1], S. A. Pérez García[2],*
F. J. Olguín Coca[1]

[1] Universidad Autónoma del Estado de Hidalgo, Carr. Pachuca Tulancingo Km 4.5, Col Carboneras, Mineral de la reforma, Hgo. México C.P. 42184
[2] Centro de Investigación en Materiales Avanzados, Miguel de Cervantes 120, Complejo Industrial Chihuahua, Chihuahua, Chih. México C.P. 31109
[*]E-mail: mveloz@uaeh.edu.mx

The electrochemical behaviour of a pyridinic compound, as corrosion inhibitor, on a system of AISI 1018 carbon steel in a synthetic corrosive medium (brine type NACE 1D196), in the absence and presence of hydrocarbon (kerosene), was investigated in this work. Electrochemical techniques used were polarisation curves and electrochemical impedance spectroscopy. In the polarization curves, it is observed that the presence of the corrosion inhibitor in the system affects both the anodic and the cathodic branches, showing that currents obtained are lower with the presence of the inhibitor. On the other hand, the inhibitor efficiency decreases with the presence of hydrocarbon in the system evaluated. Electrochemical impedance spectroscopy shows that steel has great activity in the system studied being more noticeable at low frequencies and in the presence of hydrocarbon. This shows the interaction of ions present in the solution with metal, favoured by the presence of hydrocarbon. The analysis with x-ray Photoelectron Spectroscopy (XPS) showed that the presence of hydrocarbon in the system allows the deposition of several Cl^- crystals on the metal surface. Also, there is an increase in Ca, Mg and C with a strong signal of iron, suggesting the presence of iron carbonate and iron hydroxides.

1. INTRODUCTION

The use of corrosion inhibitors has provided, for a long time, a solution to the damage caused by corrosion in the oil industry; however, due to the large number of corrosive environments, the

selection of a corrosion inhibitor is a challenging task. The number of different inhibitors available is very large and the selection depends on the metal that has to be protected, also the nature of the corrosive environment and operating conditions to which they are subjected. Currently the development of corrosion inhibitors is facing great changes and there is a real need to evaluate different compounds which have strong characteristics of corrosion inhibition and which promise to be an excellent raw material for the development of effective corrosion inhibitors in various corrosive media [1-3].
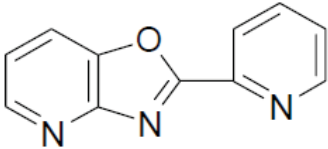
Thus, in the corrosion field it is very important understanding the corrosive characteristics of the environments within the oil industry; since the contact with metal equipment causes serious damages and the economic lost is significant [4-6]. The presence of hydrocarbon on the other hand, it is also a determining factor, due to the conditions acquired by the surface of the metallic material that can cause severe material damages leading to the loss of the entire equipment. This work is an attempt to contribute to the corrosion understanding by evaluating the electrochemical behaviour of the system AISI 1018 carbon steel-hydrocarbon- solution NACE 1D196, in the presence of an organic compound with corrosion inhibiting properties. This could serve to determine whether the efficiency and mechanism of the corrosion inhibitors is affected (and which way) by the presence of hydrocarbon.

2. EXPERIMENTAL

2.1. Organic Compound Used

The compound used is shown in Table I as well as the name given for the purposes of this paper. This compound has been used before to evaluate its inhibition in acidic media without hydrocarbon [7], indicating good inhibition properties.

Table I Compound Tested: Denomination and Chemical Structure in this paper.

Denomination	Name and Chemical Structure	
Pyridin	2-piridin-2-yl-1H-benzoimidazol	

2.2. Experimental Setup

A typical three-electrode cell setup was used in electrochemical techniques with a Hg/HgCl(s)/KCl(sat) electrode as reference and a graphite bar as counter electrode. As working electrodes, discs of low carbon steel AISI 1018 (C 0.15/0.20%; Mn 0.60/0.90%; Si 0.15/0.30%; P max.

0.04%; S max. 0.05%) were used and coupled to a Teflon support. Prior to each experiment, electrode surface was abraded with 280 SiC emery paper.

The corrosive environment used, similar to that described in the document NACE 1D196 [8], has the following composition: 0.0304M Calcium Chloride Dehydrate, 0.0101M Magnesium chloride hexahydrate and 1.824 M Sodium chloride saturated with CO_2 in the absence and presence of hydrocarbon in a ratio 8:2.

The solution was prepared with deionized water, deaerated with high purity nitrogen for 30 min. The following reagents were used (A. R. grade): 99% purity NaCl Baker; 100% purity hexahydrated $MgCl_2$ Baker, 99% purity dehydrated $CaCl_2$ Baker and kerosene (hydrocarbon) from Baker. Once the brine is prepared, it is purged with CO_2 (30 minutes per litre of brine) with a controlled pressure of 0.703 Kg/cm^2.

All experiments were performed at 49 ± 1 °C and after 10 minutes of immersion of the working electrode, allowing the corrosion potential stabilization. The potentiodynamic polarisation curves were registered at a scan rate of 0.1mV/s in a potential range between ± 300 mV (vs. o.c.p.) and each curve was obtained from a freshly abraded steel surface.

The electrochemical impedance spectroscopy (EIS) measurements were carried out with an amplitude of 10 mV (vs. o.c.p.) and in the frequency range of 10 mHz to 10 kHz. A Potentiostat-Galvanostat Autolab Mod PGSTAT30 with Frequency Response Analyser (FRA) was used and managed through the software of the same company.

It is important to stress that all electrochemical experiments were carried out under hydrodynamic conditions, using a mechanic stirrer at 2000 rpm in order to achieve a homogeneous emulsion when kerosene was introduced in the model solution.

Samples were analysed on the Thermo Scientific Escalab 250Xi using XPS, spectroscopic imaging and depth profiling. Samples were mounted on standard or cut-out holders, with conductive tape. The XR6 monochromated X-ray source was used for XPS analyses. This offers a user-selectable spot size from 200-900 µm. Automated in-lens irises may also be used to reduce the analysis area further, offering a range of 300-20 µm. In these analyses, the 900 µm X-ray spot was used for high sensitivity and rapid analysis, and to ensure good coverage in XPS imaging, and the 400 µm spot was used for depth profiling. All data processing (quantification, peak fitting, profile and image generation, PCA, average spectrum generation) was performed within the Avantage datasystem.

3. RESULTS AND DISCUSSION

3.1. Polarisation curves behaviour of the system without and with hydrocarbon

Figure 1 shows the potentiodynamic polarisation curves for the system in study under different conditions. The corrosion potential in the system is - 0.61±0.01V vs. Hg/HgCl (s) /KCl (sat) (SCE), independently of the condition used. For the system without organic compound as corrosion inhibitor, is observed that the presence of hydrocarbon affects both the anodic and cathodic branches showing greater effect on the oxidation reaction since the current is higher in comparison to the system without

hydrocarbon. On the other hand, the presence of the organic compound in the system decreases the current both in the anodic as in the cathodic branches compared to the systems in the absence of inhibitor. Similarly it is observed that the presence of hydrocarbon increases the current in comparison to the system in the absence of hydrocarbon. Also it is noteworthy to point that this behaviour was shown by other pyridinic compounds previously tested (not showed here), which exhibited a significant change in the cathodic reaction in the presence of hydrocarbon even more important than the anodic reaction so the inhibitor efficiency decreases with the presence of hydrocarbon [7]. With the results obtained here, the negative effect of the hydrocarbon is confirmed; showing that the adsorption processes are favoured by the hydrocarbon and provoking the inhibitor competence with corrosive agents in the neighbourhood of the surface. Which have been seen in previous works [7].
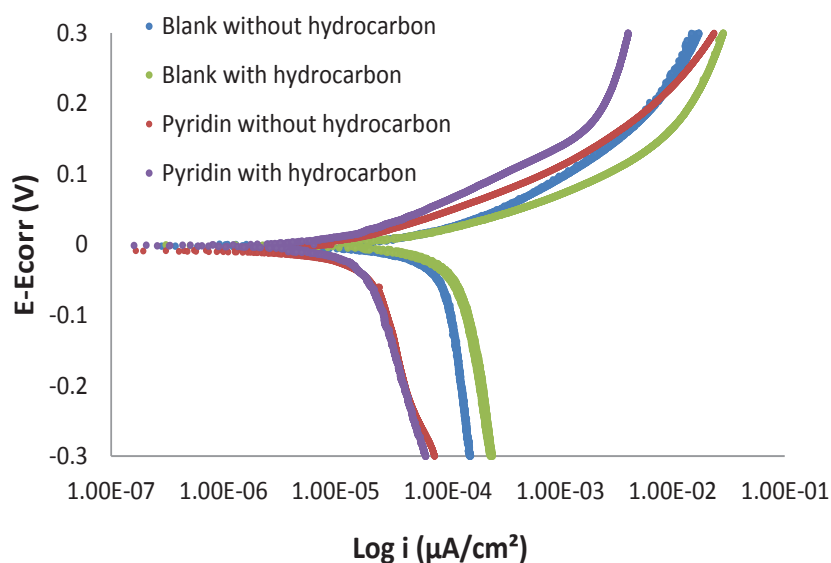

Figure 1. Polarisation curves obtained for a system of carbon steel AISI 1018 immersed in a solution NACE 1D196, the compound evaluated Pyridin and hydrocarbon.

In order to determine the values of some corrosion parameters such as the corrosion potential and Tafel slopes, an analysis of the polarisation curves was made.

3.2. Corrosion parameters for the system without and with hydrocarbon

In Table II the corrosion parameters (i.e. corrosion potential, anodic and cathodic slopes and the corrosion current) obtained from the potentiodynamic polarisation curves, are shown. Corrosion potentials obtained showed a non-significant difference between them and the value of the "blank" system, indicating that the initial energetic conditions are nearly the same.

On the other hand, analysis of the polarisation curves show that the presence of the hydrocarbon modifies the diffusive processes [9-13], since the values of anodic and cathodic slopes increase rapidly in the various systems showing non-Tafel behaviour. So, the values of

the cathodic and anodic slopes were calculated, taking into account the diffusion processes, in the range of ± 60 mV vs o.c.p., where the transfer control is assumed. Such behaviour could be attributed to the presence of a hydrocarbon film in contact with the metal surface, which is constant and that somehow favours the interaction between the compounds or corrosive species and metal [14-18].

Table II. Corrosion parameters of different systems

	Ecorr (V)	ba (V/dec)	bc (V/dec)
Blank without hydrocarbon	-0.61	0.063	-0.217
Blank with hydrocarbon	-0.61	0.074	-0.258
Pyridin without hydrocarbon	-0.60	0.033	-0.122
Pyridin with hydrocarbon	-0.60	0.058	-0.157

In order to determine in a precise way the effect of the presence of hydrocarbon on the corrosion inhibition with the compound tested, Electrochemical Impedance measurements were performed, without and with hydrocarbon.

3.3. Electrochemical Impedance behaviour of the system without and with hydrocarbon

Figure 2 shows the Nyquist diagrams as a result of the electrochemical impedance spectroscopy measurements for the system evaluating the compound as corrosion inhibitor in a concentration of 75 ppm in absence and presence of hydrocarbon.

This concentration of the inhibitor was the best in studies performed before (not showed here) [7]. The Nyquist diagrams in absence of hydrocarbon showed open semicircles and a low frequency of a linear trend indicating the presence of diffusive processes both for the system without and with inhibitor [9-11, 19-21]. On the other hand, the presence of hydrocarbon modifies the corrosion process, since the diagrams showed the appearance of flattened semicircles; also, at low frequencies a loop of inductive tendency appeared, which have been attributed to adsorption or dissolution processes that are occurring in the system [22-23]. It is worth mentioning that the presence of the organic compound increases the polarisation resistance (Rp) for each of the conditions evaluated, indicating that the process control has changed. Thus, it highlights the importance of the study since the presence of hydrocarbon in a corrosion system can promote the adsorption of corrosive species but also the corrosion inhibiting compounds.
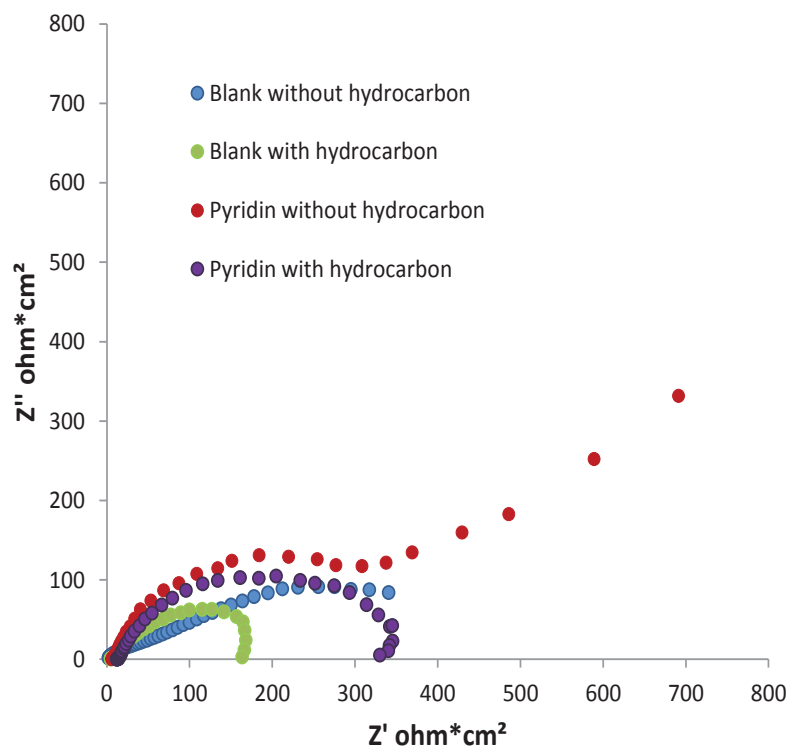
Figure 2. Nyquist diagrams for the system of carbon steel AISI 1018 immersed in a solution NACE 1D196 evaluating the compound Pyridin and hydrocarbon.

3.4. XPS behaviour of the system without hydrocarbon

For the system with Pyridin - without hydrocarbon, the sample was analysed with the magnetic lens turned off, as the sample was magnetisable. The survey spectrum (Figure 3a) shows C, O, Na, and Fe. In the case of the depth profiled (Figure 3b) using 1 keV, registered over a 2.5 x 2.5 mm area. Survey spectra were acquired at each level, for elemental concentration profiling. Peak area measurements from these survey spectra were used to generate a depth profile. The depth scale was calibrated by sputtering a 30 nm Ta_2O_5/Ta foil sample under the same conditions. Surface carbon is removed rapidly, but carbon persisted over 10 nm into the sample. Oxygen is removed slowly, and iron increases in intensity. Sodium and manganese are roughly constant in intensity through the profile, while calcium seems to increase slightly.

3.4. XPS behaviour of the system with hydrocarbon

For the system with Pyridin and hydrocarbon the sample was analysed with the magnetic lens turned off, as the sample was magnetisable. The survey spectrum (Figure 4a) from a lighter area shows C, O, Na, and Fe, along with several other low-concentration elements. In the case of the depth profiled (Figure 4b) using 1 keV Ar ions, registered over a 2.5 x 2.5 mm area. Survey spectra were acquired at each level, for elemental concentration profiling. Peak area measurements from these survey spectra were used to generate a depth profile. The depth scale was calibrated by sputtering a 30

nm Ta$_2$O$_5$/Ta foil sample under the same conditions. Surface carbon is removed rapidly, but carbon persisted deep into the sample. Oxygen is removed slowly, and iron increases in intensity. Lead is a surface species, and is removed entirely after a few etch cycles. Manganese is roughly constant in intensity through the profile, while sodium, calcium and chlorine all fall slightly.
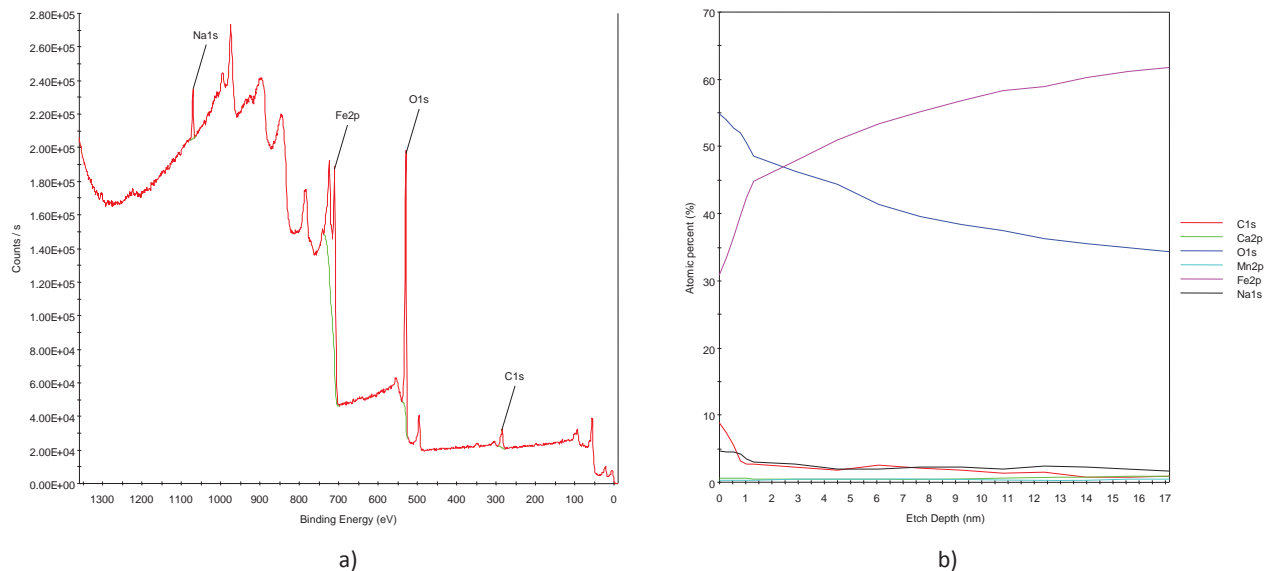

a)   b)

Figure 3. XPS a) Survey Spectrum and b) Depth Profile for the system of carbon steel AISI 1018 immersed in a solution NACE 1D196 evaluating the compound Pyridin without hydrocarbon.
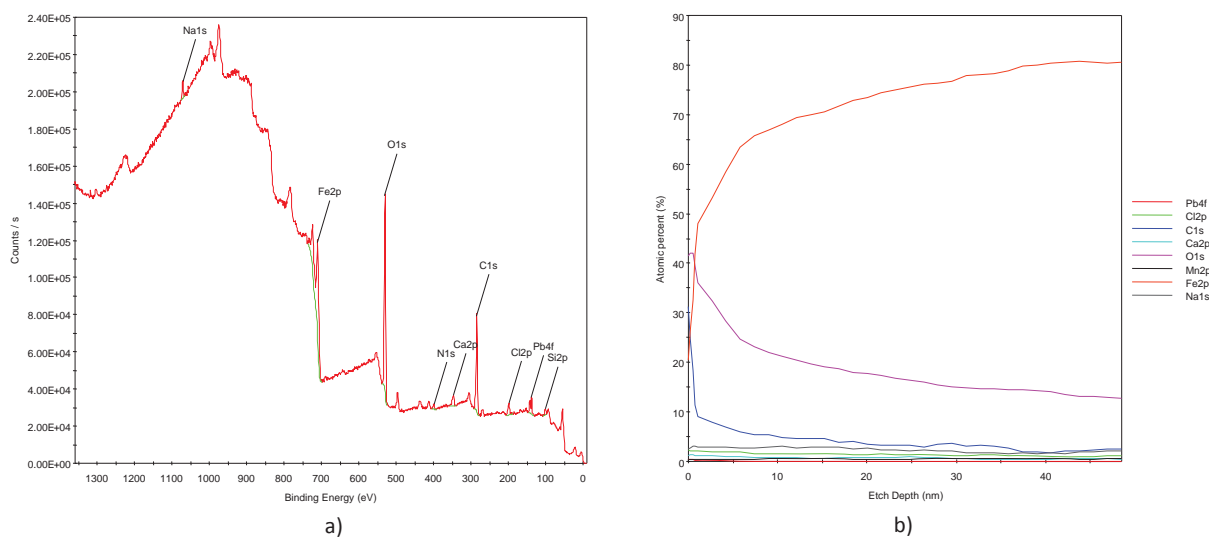

a)   b)

Figure 4. XPS a) Survey Spectrum and b) Depth Profile for the system of carbon steel AISI 1018 immersed in a solution NACE 1D196 evaluating the compound Pyridin with hydrocarbon.

For the system Pyridin - with hydrocarbon Parallel XPS images (Figure 5) were acquired from the crystal-covered area, in an attempt to identify the crystal chemistry. Peak-Background images were acquired for each element. NaKLL and MgKLL were used in preference to Ma1s and Mg1s as the peak: background signal ratios are preferable at the Auger peak energies. The images show that several of the crystals, including the square one in the centre, are NaCl. In the central region that is not covered by crystals, there is an increase in Ca, Mg and C, which may be deposition of salts. Near the top, where there is a band of brown crystals visible in the camera image, the iron signal is quite strong, suggesting that these crystals are Fe-rich. It is possible that these crystals are iron carbonate or hydroxide [24].
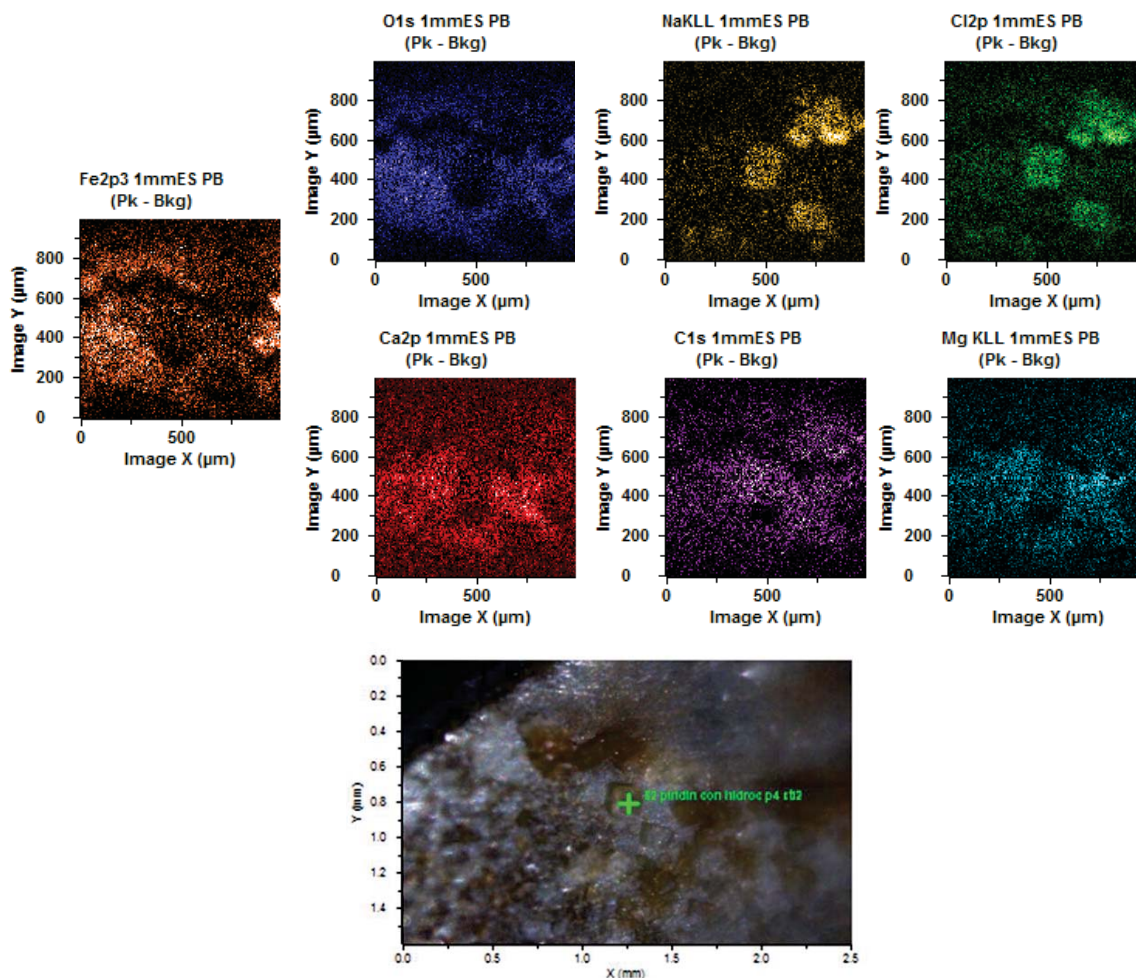

Figure 5. Parallel XPS Imaging for the system of carbon steel AISI 1018 immersed in a solution NACE 1D196 evaluating the compound Pyridin with hydrocarbon.

4. CONCLUSIONS

In potentiodynamic polarisation curves, the presence of hydrocarbon affects both the anodic and the cathodic branches, showing that the currents obtained are higher for the different systems (with

and without inhibitor). The inhibition efficiency decreases with the presence of hydrocarbon in the system showing an increase in the currents, however, the diffusive processes are still present in the system.

The use of electrochemical impedance spectroscopy technique shows that the interaction of the hydrocarbon modifies the corrosion process; also, it is observed that there are adsorptive processes favouring the arrival of corrosive agents to the metal surface.

Through XPS is observed that interaction of chlorides with metal under different conditions, is increased with the presence of hydrocarbon by considerably modifying the corrosion rate of the system; moreover, the adsorption stages governing the corrosion process, are also favoured.

References

1. B. R. Álvarez, S. G. Negrón, Q. M. Abreu, H.H. Herrera, M. Romero, A. Cuán., P. M. Palomar., *Electrochimica Acta*, 54, (2009) 5393
2. Z.A. Foroulis, *"Role of solution pH on wet H_2S cracking in hydrocarbon production"*, Corrosion Prevention & Control, (1993) 84
3. I. V. Sieber, H. Hildebrand, S. Virtanen, P. Schmuki., *Corros Sci* 48 (2006) 3472
4. M.A. Veloz, I. Gonzalez, *Electrochim. Acta,* 48 (2002) 135
5. Kedam M., Mattos O. R., Takenouti H., *J. Electrochem. Soc*. 128 (1981) 257
6. Q. Qu, L. Li, S. Jiang, W Bai, Z. Ding, *J. Appl. Electrochem.* 39 (2009) 569
7. L. D. López, M. A. Veloz, V.E. Reyes, S.A. Pérez, A. L. López, *Int. J. Electrochem. Sci*. 6 (2011) 5134-5145
8. Method NACE 1D196 *"Laboratory Test Methods for Evaluating Oilfield Corrosion Inhibitors"*, NACE, (1996)
9. R.E. Melchers, *Corros. Sci.* 45 (2003) 2609
10. M. M. Singh, A. Gupta, *Corrosion,* 56 (2000) 371
11. K. Magne, *J. of Disp. Sci. and Tech*. 27 (2006) 587
12. A. Nagiub, F. Mansfeld, *Corros. Sci.* 43 (1987) 2147
13. H. Ma, X. Cheng, G. Li, S. Chen, Z. Quan, S. Zhao, L. Niu, *Corros. Sci*.42 (2000) 1669
14. M.G. Hosseine, M. Ehteshamzadeh and T. Shahrabi : *Electorchim. Acta*, 25 (2007)3680
15. H.E. El Ashry, A. El Nemr, S.A. Esawy, S. Ragab, *Electrochimica Acta* 51 (2006) 3957
16. G.Z. Meng, *Corros. Sci*. 50 (2008) 3116
17. A.K. Singh, M.A. Quraishi, *Corros. Sci*. 53 (2011) 1288
18. J.K. Heuer, J.F. Stubbings, *Corrosion*, 54 (1998) 566
19. A.M. Alsabagh, M.A. Migahed , and H.S. Awadi., *Corros. Sci*., 48 (2006) 813
20. A. Benmoussat, M. Hadjel, *Journal of Corrosion Science and Engineering*, 7 (2005) 14
21. H Ashassi, T.A Aliyev, S Nasiri, R Zareipoor, *Electrochim. Acta*, 52 (2007) 5238
22. G.E. Badr, Corros. Sci. 51 (2009) 2529
23. S. Ghareba and S. Omanovic, *Corros. Sci*., 52 (2010) 2104
24. F. Bentiss, M. Traisnel, L. Gengembre, M. Lagrenée, *Appl. Surf. Sci.* 161 (2000) 194